Journal of Materials Chemistry B

RSC Publishing

PAPER

View Article Online
View Journal | View Issue

Cite this: *J. Mater. Chem. B*, 2013, **1**, 2245

Functionalization of dendritic polyethylene with cationic poly(*p*-phenylene ethynylene) enables efficient siRNA delivery for gene silencing

Ling Zhang,* Qi-He Yin, Jin-Ming Li, Hong-Ying Huang, Qing Wu and Zong-Wan Mao

Received 3rd December 2012
Accepted 21st February 2013

DOI: 10.1039/c3tb00480e

www.rsc.org/MaterialsB

A novel system based on a dendritic polyethylene–cationic poly(*p*-phenylene ethynylene) polyvalent nanocarrier was developed for siRNA delivery. By using the combination of a molecular wire and a "dendritic effects" strategy, this design provides the nanocarrier system with low cytotoxicity, cellular imaging and high siRNA delivery efficiency, allowing it to exhibit remarkable gene knockdown abilities as well as real-time monitoring of the siRNA delivery process.

Introduction

Recently, short interfering RNA (siRNA) has been considered as a new class of nucleic acid therapeutic for treatment of various infectious and genetic diseases including cancer *via* RNA interference (RNAi).[1] A successful approach used for siRNA delivery *in vitro* and *in vivo* involves the formation of ionic complexes (polyplexes) through noncovalent interaction between the negatively charged phosphate groups in siRNA and the cationic charges in the macromolecular vectors such as lipids,[2a] dendrimers,[2b,c] and polymers.[2d–h]

Despite these intense studies, effective delivery of siRNA to target cells under *in vivo* conditions still remains a significant challenge to realizing its full therapeutic potential due to their low tolerability under physiological conditions and poor cellular uptake.[3] Furthermore, it would be difficult to observe the siRNA delivery process, which is very useful for RNAi therapy investigation, because these delivery systems usually lack intrinsic fluorescence. While quantum dots (QDs) have been reported as siRNA carriers for high efficiency and monitored siRNA delivery,[4] the cytotoxicity of the QDs must be considered if using this kind of siRNA delivery system *in vivo*. Thus, the development of a low cytotoxicity, high efficiency and monitored system for siRNA delivery is essential.

In Segura and Guo's review papers,[5] they have highlighted biocompatible polyvalent nanocarriers as delivery vehicles for siRNA delivery. Meanwhile, some biocompatible polyvalent nanocarriers based on the tunable surface charge of gold nanorods have been applied in siRNA delivery.[6] Most of all, water-soluble cationic conjugated polyelectrolytes provide an excellent polyvalent scaffold for siRNA delivery, since cationic conjugated polyelectrolyte chains with multiple recognition elements can bind to the negatively charged siRNA through electrostatic interactions. Moreover, water-soluble cationic conjugated polyelectrolytes feature efficient optical signal transduction and high resistance to photobleaching,[7–9] allowing them to monitor the siRNA delivery process. However, no methods have been developed for utilizing fluorescent conjugated polyelectrolyte-based polyvalent nanoparticles and their unusual properties to load and transport siRNA across cell membranes.

Among them, water-soluble poly(*p*-phenylene ethynylene) (PPEs) with synthetic versatility are especially attractive fluorescence probes for sensing cells, imaging living cells and cancer cells *in vitro*.[10–13] In spite of these promising properties, even charged PPEs have a strong tendency to aggregate which results in subsequent fluorescent quenching in aqueous solution,[14] which presents a major bottleneck for siRNA delivery and intracellular imaging. We have developed a method for synthesizing dendritic polyethylene–cationic poly(*p*-phenylene ethynylene) (DPE–PPE$^+$) core–shell nanoparticles with small size, biocompatibility and good cellular permeability.[15]

In this work, polyvalent nanocarriers based on dendritic polyethylene–cationic poly(*p*-phenylene ethynylene) (DPE–PPE$^+$) were investigated as siRNA carriers to target silencing of VEGF protein in HeLa cells. In comparison with efficient uptake of the target cells, folic acid (FA) ligands may be introduced on the shell of DPE–PPE to obtain water-soluble DPE–PPE–FA$^+$. We expect that these polyvalent nanocarriers will not only deliver siRNA much more effectively for gene silencing, but also will be applicable to the observation of the siRNA delivery process.

DSAPM Lab, PCFM Lab, OFCM Institute, MOE Key Laboratory of Bioinorganic and Synthetic Chemistry, School of Chemistry and Chemical Engineering, Sun Yat-Sen University, Guangzhou 510275, China. E-mail: ceszl@mail.sysu.edu.cn

Experimental

Materials and general methods

All chemicals and solvents were purchased from Sigma-Aldrich or Acros Organics, and used without further purification unless otherwise noted. HeLa cells were obtained from the Experimental Animal Center of Sun Yat-sen University.[15] The anti-VEGF antibody and β-actin monoclonal antibody were obtained from Santa Cruz (USA). VEGF siRNA (siVEGF) was purchased from Dharmacon (USA) including Cy3-labeled siRNA (siRNA^{Cy3}). siRNA^{Cy3} has the sequences of 5′-CCUACGCCAAUUUC GUdTdT-3′ (sense) and 5′-ACGAAAUUGGUGGCGUAGGdTdT (antisense). The siRNA was labeled with Cy3 at the 5′-end of its sense strand. The sequences of siVEGF were 5′-AUGUGAAU GCAGACCAAAGAATT-3′ (sense) and 3′-TTUAACACUUACGUCU GGUUUCUU-5′ (antisense). All NMR spectra were recorded at 25 °C on a Varian Mercury-Plus 300 M or a Varian Inova 500 M spectrometer in D_2O or DMSO-d_6 with reference to solvent residual peaks or TMS. Cytotoxicity assay was described in our previous report.[15]

Synthesis of DPE–PPE$^+$ and DPE–PPE–FA$^+$

The dendritic macromonomer bearing multiple iodine groups (DPEI) was synthesized using the Brookhart palladium–α-diimine chain walking catalyst. Based on DPEI, a neutral DPE–PPE was synthesized by palladium/copper-catalyzed Sonogashira cross-coupling. Moreover, quaternization of DPE–PPE was conducted with bromoethane to obtain the water-soluble cationic DPE–PPE (DPE–PPE$^+$). The detailed synthesis of DPE–PPE$^+$ was described in our previous work.[15] *N*-Hydroxysuccinimide ester of folic acid (FA-NHS) was prepared in accordance to a reported procedure.[16,17] Vacuum-dried FA-NHS was then dissolved in 1.5 mL of a mixture of DMSO and TEA with a volume ratio of 2 : 1. An equal molar amount of 2-aminoethanebromine was added to the mixture, and the reaction was conducted under anhydrous conditions overnight.[17,18] Therefore, a bromine group was introduced into folic acid to form FA–Br by nucleophilic substitution (Scheme 1). ^{1}H NMR of FA–Br (DMSO-d_6) δ 8.61 (s, 1H), 8.06 (d, 1H), 7.62 (d, 2H), 7.42 (d, 1H), 7.21 (t, 1H), 6.91 (br), 6.60 (d, 2H), 5.56 (d, 1H), 4.48 (d, 2H), 4.20 (m, 1H), 3.06 (t, 1H), 2.99 (q, 1H), 2.53 (mm, 4H), 2.30 (t, 1H), 2.10–1.85 (mm, 2H). Moreover, quaternization of the neutral DPE–PPE with a mixture of FA–Br and bromoethane was conducted to obtain DPE–PPE–FA$^+$ in the same way as the previous description of DPE–PPE$^+$.[18,19]

The formation of DPE–PPE$^+$/siRNA and DPE–PPE–FA$^+$/siRNA complexes

The DPE–PPE–FA$^+$/siRNA complex was prepared by mixing siRNA with the specified amount of DPE–PPE–FA$^+$ solution followed by incubation in serum-free medium at room temperature for 15 min. The weight ratio of DPE–PPE–FA$^+$ to siRNA varied from 4 to 32. The complex formation was confirmed by agarose gel electrophoresis. The siRNA and DPE–PPE–FA$^+$/siRNA complexes were loaded in the wells of 1.0 wt% agarose gel containing ethidium bromide (EtBr) at a concentration of 0.5 ug mL^{-1}, to which was applied 190 V electrodes in 1× TBE buffer (pH 9) for 10 min. The siRNA was visualized by EtBr staining and the gel image was taken under UV. The gel electrophoresis of DPE–PPE$^+$/siRNA complex was conducted in the same way as described above for the DPE–PPE–FA$^+$/siRNA complex.

siRNA protection of DPE–PPE$^+$ and DPE–PPE–FA$^+$ nanocarriers

To study the ability of nanocarriers in protection of loaded siRNA from being degraded by RNaseA, DPE–PPE$^+$/siRNA and DPE–PPE–FA$^+$/siRNA complexes were formed following the procedure described above. Next, 10 unit RNaseA was added to the complexes, and the resulting mixtures were incubated at 37 °C for 90 min. After incubation, 1 μL of 50 U μL^{-1} RNaseA inhibitor was added to stop the degradation reaction, and then 3 μL of 1% SDS was added to dissociate the siRNA from the complexes. The gel electrophoresis images were taken under a UV illuminator, and the results were analyzed to identify the remains of siRNA after the degradation of RNaseA, and compared with naked siRNA in the presence of RNaseA. A parallel experiment was conducted as a control for naked siRNA in the absence of RNaseA.

Flow cytometric analysis

HeLa cells were grown in DMEM containing 10% FBS at 37 °C in a 5% CO_2 atmosphere. Six-well plates (Corning Inc., Corning, NY) were used with a well volume of 2.6 mL. The cells were trypsinized, counted, and adjusted to 1 × 10^5 cells per mL and

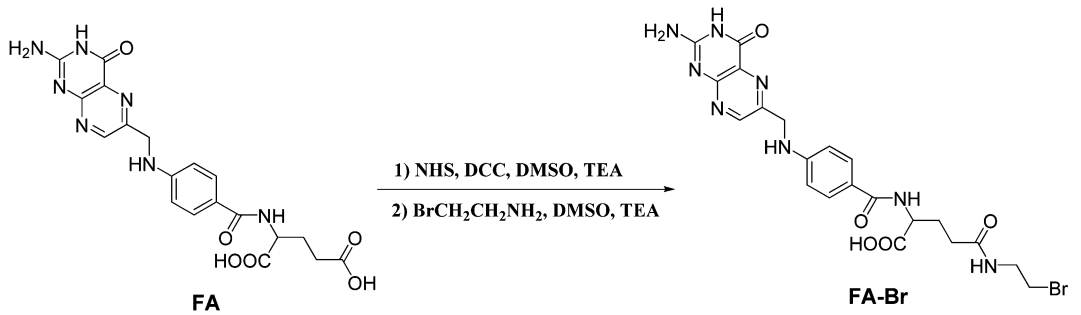

Scheme 1 Synthesis of FA–Br.

1 mL was added per plate. Stock solutions of DPE–PPE$^+$, DPE–PPE–FA$^+$ and their siRNA complexes were diluted using DMEM and added to the plate in 20 μL quantities (c = 50 μg mL^{-1}). After incubation for 6 h, cells were thoroughly washed with PBS three times in order to eliminate DPE–PPE$^+$, DPE–PPE–FA$^+$ and their siRNA complexes that were not internalized. The cells were trypsinized and centrifuged in PBS buffer. Then the DPE–PPE$^+$, DPE–PPE–FA$^+$ and their siRNA complex bound cells were harvested and a single cell suspension in 0.5 mL PBS buffer was prepared and subjected to flow cytometric analysis. A flow cytometer (Coulter Co. USA) was used to measure the fluorescence intensity with excitation at 488 nm.

Laser confocal microscopy image analysis

For achieving confocal images, HeLa cells were seeded in a laser confocal microscopy 35 mm^2 Petri dish (MatTek, USA) at a density of 1.0 × 10^5 cells and stored for 48 h. DPE–PPE–FA$^+$/siRNA was prepared in serum-free media and incubated for 15 min at room temperature. The media containing serum were added into the solution, and cells were transfected with the complex and incubated for different time intervals (2 h and 5 h). After the transfection, the media were discarded and the cells were washed 3 times with 1× PBS. Confocal images were obtained at each time point using a Leica TCS SP5 confocal laser scanning microscope (Leica Inc., USA). To acquire the fluorescence signal, each sample was excited at 488 nm with an Ar laser. A fluorescence signal of siRNA^{Cy3} was detected at 570–600 nm and the DPE–PPE–FA$^+$ signal was obtained at 480–510 nm with excitation at 488 nm.

Cell transfection procedures

Cellular transfection of siRNA was performed using DPE–PPE$^+$ and DPE–PPE–FA$^+$ and commercial transfection reagents (siPort NeoFX, Ambion Inc, USA; HiPerFect, Qiagen Inc, Germany). For siRNA transfection, cells were trypsinized with 0.25% of trypsin solution (HyClone Inc, USA) for 3 min at 37 °C. Next, 1 × 10^4 cells per well were plated into 24-well plates (Corning Inc, USA) overnight to achieve 60–80% confluence. On the day of transfection, cultured cells were washed with 1× PBS and incubated for 30 min with DMEM without serum and antibiotics. siPort NeoFX (2 μL per well) and HiPerFect (2 μL per well) were diluted in 500 μL of DMEM (manufacturer recommended concentrations) and were incubated for 15 min at room temperature. Then 100 nM siRNA against VEGF (Dharmacon Inc, USA) was added to the mixture of medium and transfection agents and incubated for an additional 20 min at room temperature. Immediately before transfection, 500 μL of DMEM were added to DPE–PPE$^+$/siRNA, DPE–PPE–FA$^+$/siRNA complexes and were mixed by pipetting. The DPE–PPE$^+$/siRNA, DPE–PPE–FA$^+$/siRNA complexes diluted in DMEM were then added to each well, and the cells were incubated at 37 °C for 24 h. DMEM with 10% FBS was then added to the cells and incubated for 24 h at 37 °C in a CO_2 incubator. After 24 h, the protein was extracted from the transfected cells for Western blotting.

Western blotting

Transfected cells and untransfected controls were lysed using M-PER® protein extraction reagent (Pierce Inc, USA). The lysates were separated by centrifugation at 12k rpm, 4 °C for 10 min on an Eppendorf 5417R centrifuge (Eppendorf Inc, Germany). Supernatants were then collected, and the protein concentration was measured by a standard BCA protein assay kit (Novagen Inc, USA). Equal amounts of protein were loaded and separated on 12% sodium dodecyl sulfate polyacrylamide gel electrophoresis (SDS-PAGE) and were then transferred for 1 h at 150 V using Bio-Rad Mini-PROTEAN4 (Bio-Rad Inc, USA) to nitrocellulose membranes (Bio-Rad Inc, USA) in transfer buffer (25 mM Tris–HCl, 200 mM glycine, 10% methanol) and blocked with 5% milk blocking buffer for 2 h on a horizontal shaker. The blocked membranes were incubated with 1 : 1000 rabbit antihuman VEGF antibody (Santa Cruz Inc, USA) diluted in 5% milk blocking buffer. The membranes were washed in Tween-Tris Buffered Saline (TTBS: 0.1% Tween-20 in 100 mM Tris–HCL [pH 7.5], 0.9% NaCl) and probed with secondary antibody (goat antirabbit IgG conjugate HRP) diluted at 1 : 5000 in 5% milk blocking buffer. The blots were developed by using an ECL kit (Amersham Inc, USA). The membranes were exposed to Kodak X-OMAT film for 10–30 s for data acquisition and developed using a conventional film developing machine.

Statistical analysis

Statistical analysis of data was performed with the one-factor analysis of variance (SPSS software, version 13.0, SPSS Inc). The results were expressed as mean ± SD (standard deviation), and $P < 0.05$ was considered to be statistically significant. All statistical tests were two-sided.

Results and discussion

For this study, we utilized cationic ammonium PPE as nonspecific binding element for siRNA, which was spatially restricted by the DPE framework. As showed in Scheme 2, a neutral DPE–PPE was synthesized by a tandem polymerization methodology, chain walking polymerization (CWP) followed by palladium/copper-catalyzed Sonogashira cross-coupling. The water-soluble cationic DPE–PPE (DPE–PPE$^+$) was obtained through quaternization of its neutral polymer.[15] The quaternization degrees (QDs) of DPE–PPE$^+$ could be estimated to be about 50% by ^{1}H NMR spectroscopy (Fig. 1), suggesting that almost half of all side chains featured a tertiary amino group.[20] In an attempt to develop a siRNA nanocarrier with more efficient uptake of the target cells, FA ligands may be installed on the periphery of the PPE palisade of DPE–PPE to obtain water-soluble DPE–PPE–FA$^+$ through a FA–Br-mediated quaternization pathway. Coupling of the folate residue to the periphery of the PPE palisade of DPE–PPE$^+$ was confirmed by the appearance of signals at δ 6.0–9.0 ppm in the magnified ^{1}H NMR spectrum of DPE–PPE–FA$^+$ (Fig. 1), which corresponded to the aromatic protons of folic acid. This is consistent with the ref. 16 and 17. The relevant signals of folate are much weaker than the broad and strong proton signals of PPE$^+$.

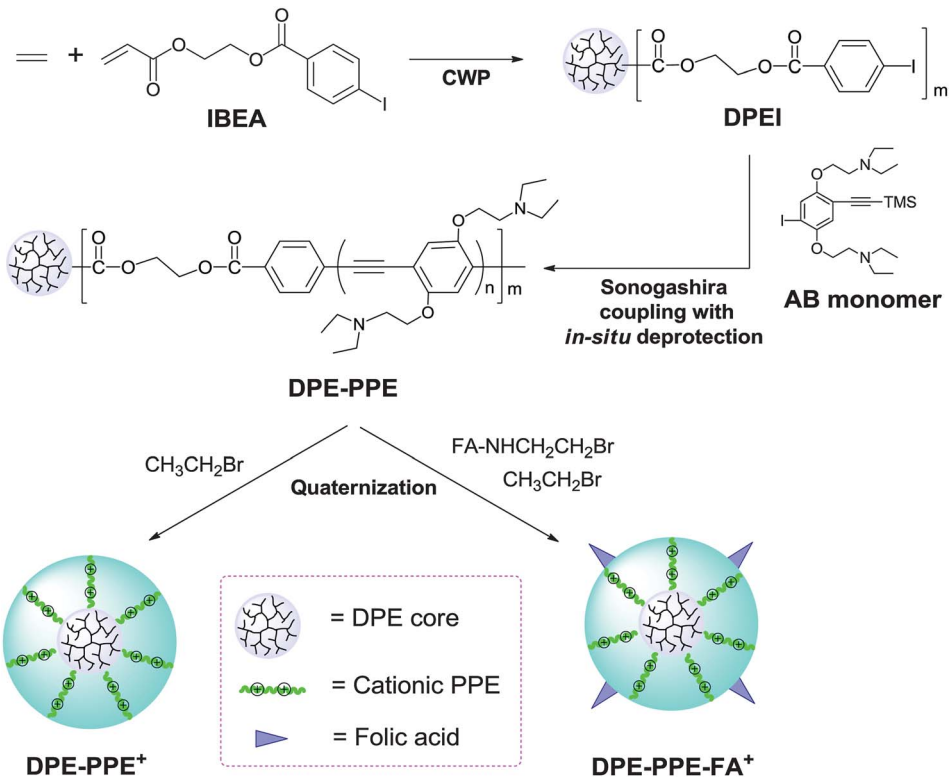

Scheme 2 Synthetic routes for DPE–PPE$^+$ and DPE–PPE–FA$^+$.

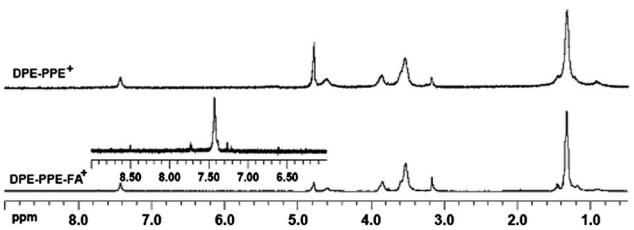

Fig. 1 ^{1}H NMR spectra of DPE–PPE$^+$ and DPE–PPE–FA$^+$ in D_2O.

Cytotoxicity of DPE–PPE$^+$ and DPE–PPE–FA$^+$

To evaluate the applicability of DPE–PPE$^+$ and DPE–PPE–FA$^+$ in live cell studies, we assessed their acute cytotoxicity as a function of their concentration by standard MTT assay in HeLa cells. After 48 h treatment, the viability of HeLa cells was more than 80% at concentrations ranging from 0 to 200 μg mL^{-1} for DPE–PPE$^+$ (Fig. 2). For comparison with DPE–PPE$^+$, a similar cytotoxicity result of DPE–PPE–FA$^+$ was obtained, suggesting that the introduction of FA on the surface of the nanocarrier has little effect on the cell viability for DPE–PPE–FA$^+$. The results demonstrate that both DPE–PPE$^+$ and DPE–PPE–FA$^+$ have significantly low cytotoxicity and have potential applications for *in vivo* siRNA delivery.

The formation of DPE–PPE$^+$/siRNA and DPE–PPE–FA$^+$/siRNA

In this study, DPE–PPE$^+$ and DPE–PPE–FA$^+$ were investigated as siRNA carriers. The formation of DPE–PPE–FA$^+$/siRNA complex by

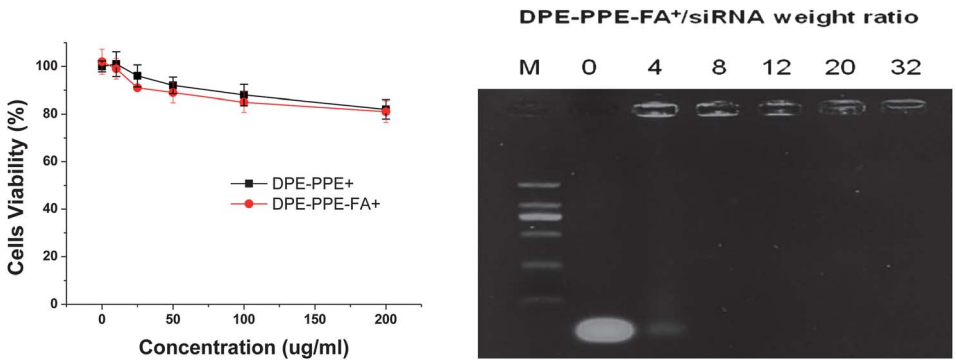

Fig. 2 Cell cytotoxicity of DPE–PPE$^+$ and DPE–PPE–FA$^+$ in HeLa cells by MTT (left) and agarose gel electrophoresis of DPE–PPE–FA$^+$/siRNA complex with various ratios of DPE–PPE–FA$^+$ conjugate to siRNA (right).

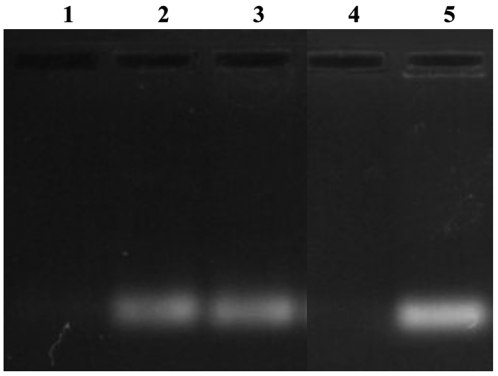

Fig. 3 The protection effect of DPE–PPE$^+$ and DPE–PPE–FA$^+$ carriers on siRNA in the presence of RNaseA. Protection of siRNA exposed to RNaseA for 90 min was measured for DPE–PPE$^+$/siRNA (lane 2) and DPE–PPE–FA$^+$/siRNA (lane 5) complexes, and compared with naked siRNA in the presence of RNaseA (lanes 1 and 4). Lane 3 corresponds to control naked siRNA in the absence of RNaseA.

the electrostatic interaction between negatively charged siRNA and positively charged DPE–PPE–FA$^+$ conjugate was assessed by agarose gel electrophoresis (Fig. 2). The DPE–PPE–FA$^+$/siRNA complex appeared to be formed when the weight ratio of DPE–PPE–FA$^+$ conjugate to siRNA was higher than 20. A similar result was obtained for the formation of DPE–PPE$^+$/siRNA complex. Thus the optimized weight ratios of DPE–PPE$^+$/siRNA and of DPE–PPE–FA$^+$/siRNA were determined to be 20 : 1 in the preparation experiments, therefore these values were selected for further work.

siRNA protection of DPE–PPE$^+$ and DPE–PPE–FA$^+$ nanocarriers

As we know, siRNA can be easily degraded by nucleic acidase, which has hindered the application of siRNA as tools in gene silencing to some extent. Therefore, the capability to protect siRNA is very important for the carrier. The siRNA protection

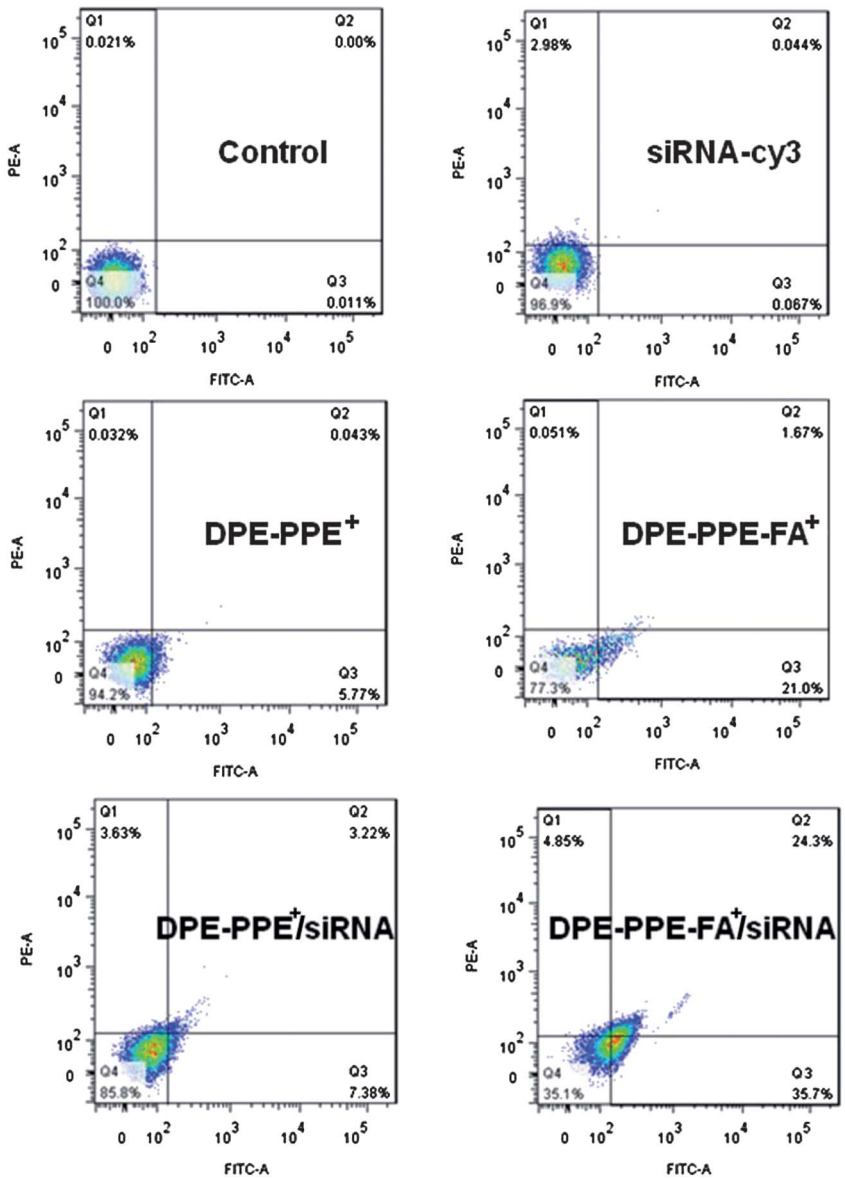

Fig. 4 Flow cytometry for transfection of DPE–PPE$^+$/siRNA, DPE–PPE–FA$^+$/siRNA and the control. Incubation time: 6 h. Dose: 100 nM siRNA^{Cy3}.

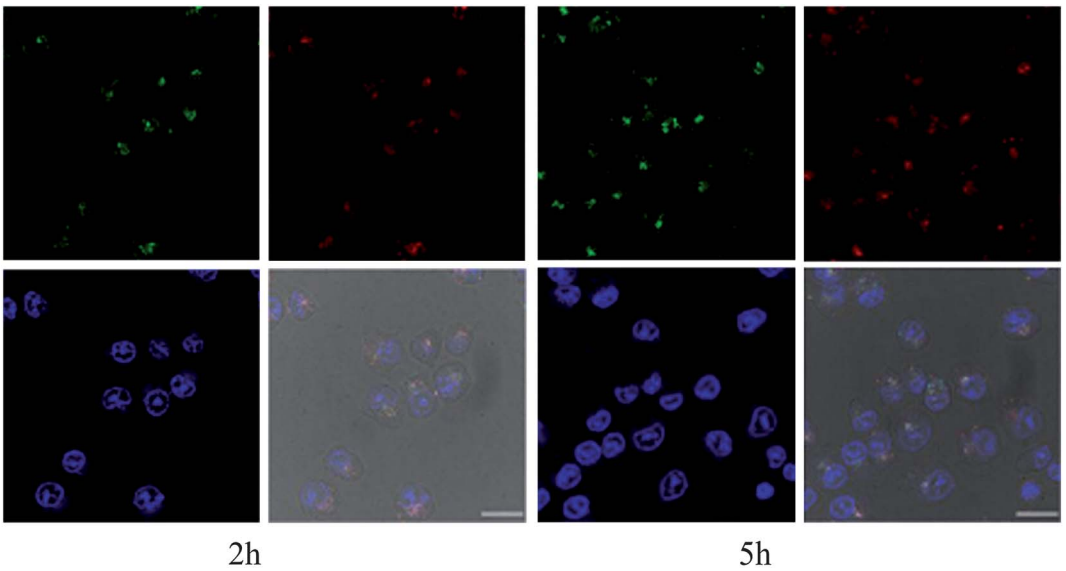

Fig. 5 Time-dependent confocal microscopy images of DPE–PPE–FA$^+$/siRNA complexes and their entry and transportation in HeLa cells. The red florescence is siRNA^{Cy3} and the green florescence is DPE–PPE–FA$^+$. Scale bars: 25 μm.

experiment was performed to measure the capability of the DPE–PPE$^+$ and DPE–PPE–FA$^+$ carriers to protect siRNA from being degraded by RNaseA. As shown in Fig. 3, naked siRNA was completely degraded under the experimental conditions (Fig. 3, lanes 1 and 4). However, siRNA bound within the carriers was stable to RNaseA over a 90 min incubation at 37 °C (Fig. 3, lanes 2 and 5), suggesting the conjugation of siRNA to DPE–PPE$^+$ and DPE–PPE–FA$^+$ carriers could both effectively protect siRNA from enzymatic degradation.

Intracellular uptake of DPE–PPE$^+$/siRNA and DPE–PPE–FA$^+$/siRNA complexes

Flow cytometry was utilized to evaluate transfer efficiency when using DPE–PPE$^+$ and DPE–PPE–FA$^+$ as nanocarriers to deliver siRNA^{Cy3} into HeLa cells (Fig. 4). According to the quantitative flow cytometric analysis, DPE–PPE–FA$^+$ showed greater uptake than DPE–PPE$^+$ in HeLa cells at the same concentrations, suggesting the FA on the surface of nanocarrier could make the entry of the nanocarrier into the targeted cells easier. It was also shown that DPE–PPE$^+$ and DPE–PPE–FA$^+$ nanocarriers displayed siRNA transfer activity. Cationic conjugated polymer chains with multiple recognition elements can bind to the negatively charged siRNA through electrostatic interactions, thereby increasing the delivery efficiency of siRNA. Moreover, siRNA was more efficiently transferred into cells when using DPE–PPE–FA$^+$ rather than DPE–PPE$^+$, as shown in Fig. 4.

Considering that DPE–PPE–FA$^+$ as siRNA nanocarrier exhibited better results than DPE–PPE$^+$, we chose confocal microscopy to monitor the time-dependent accumulation of DPE–PPE–FA$^+$/siRNA complex in HeLa cells (Fig. 5). After internalization, the DPE–PPE–FA$^+$/siRNA complexes were observed to become accumulated at a region outside the cell nucleus at 2 h. Cellular uptake of more complexes was observed and more siRNAs were transported into the cells at 5 h. It is shown that DPE–PPE–FA$^+$ nanocarrier exhibits efficient cellular uptake, and rapid transport of siRNA into the cell. Like QD particles, the intrinsic fluorescence of DPE–PPE$^+$ and DPE–PPE–FA$^+$ renders them well-suited for the observation of the siRNA delivery process, but they have lower cytotoxicity than QD particles.

Gene silencing efficiency of DPE–PPE$^+$/siRNA and DPE–PPE–FA$^+$/siRNA complexes

The gene silencing efficiency of DPE–PPE$^+$ and DPE–PPE–FA$^+$ were investigated by western blotting experiments, and commercial transfection reagents, siPort NeoFX and HiPerFect were kept as contrasts (Fig. 6). The results showed similar silencing efficiencies of DPE–PPE$^+$ and DPE–PPE–FA$^+$ on VEGF protein in HeLa cells after transfection compared with the commercial transfection reagents. Compared with the controls, the levels of VEGF protein expression were reduced to 18 ± 8.5%

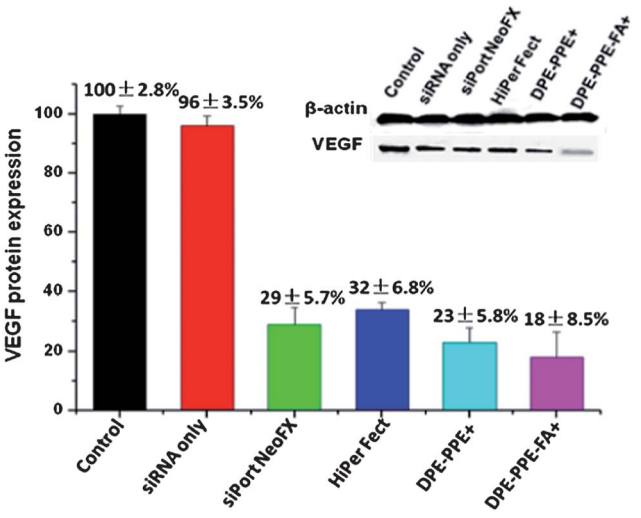

Fig. 6 The suppression of VEGF protein expression was evaluated by western blotting. The siRNA carriers are DPE–PPE$^+$ and DPE–PPE–FA$^+$ ($n = 3$; $p < 0.05$).

and 23 ± 5.8% for DPE–PPE–FA$^+$ and DPE–PPE$^+$ treated cells, respectively. Using DPE–PPE$^+$ and DPE–PPE–FA$^+$ as siRNA nanocarriers, we achieved gene silencing efficiency of almost 80% in HeLa cells. It is shown that an appreciable silencing of the target gene at an extremely low siRNA concentration is achieved through the assembly of siRNA into smart DPE–PPE$^+$ and DPE–PPE–FA$^+$ polyvalent nanoparticles.

Conclusions

We report here an effective monitored siRNA delivery system based on the water-soluble dendritic polyethylene–cationic poly(*p*-phenylene ethynylene). For utilizing fluorescent conjugated polyelectrolyte-based polyvalent nanocarriers and their unusual properties to load, protect and transport siRNA across cell membranes, the distinctive nanocarrier design achieved low cytotoxicity, high transfer efficiency and monitored siRNA delivery. Notably, the complex of the nanocarrier system and siRNA revealed remarkable gene knockdown. These results suggest that this newly designed system of polyvalent nanocarriers will have great promise for *in vivo* gene therapeutics.

Acknowledgements

This work was financially supported by the program of National Natural Science Foundation of China (Grant no. 20804059.), and the Fundamental Research Funds for the Central Universities (Grant no. 31000-3161711).

Notes and references

1 (*a*) A. Fire, S. Xu, M. K. Montgomery, S. A. Kostas, S. E. Driver and C. C. Mello, *Nature*, 1998, **391**, 806; (*b*) S. M. Elbashir, J. Harborth, W. Lendeckel, A. Yalcin, K. Weber and T. Tuschl, *Nature*, 2001, **411**, 494; (*c*) H. Kawasaki and K. Taira, *Nucleic Acids Res.*, 2003, **31**, 700; (*d*) T. P. O'Connor and R. G. Crystal, *Nat. Rev. Genet.*, 2006, **7**, 261; (*e*) M. A. Kay, *Nat. Rev. Genet.*, 2011, **12**, 316; (*f*) C. Sheridan, *Nat. Biotechnol.*, 2011, **29**, 121; (*g*) A. Reynolds, D. Leake, Q. Boese, S. Scaringe, W. S. Marshall and A. Khvorova, *Nat. Biotechnol.*, 2004, **22**, 326; (*h*) D. Bumcrot, M. Manoharan, V. Koteliansky and D. W. Y. Sah, *Nat. Chem. Biol.*, 2006, **2**, 711; (*i*) A. de Fougerolles, H. P. Vornlocher, J. Maraganore and J. Lieberman, *Nat. Rev. Drug Discovery*, 2007, **6**, 443; (*j*) D. H. Kim and J. J. Rossi, *Nat. Rev. Genet.*, 2007, **8**, 173; (*k*) J. Kurreck, *Angew. Chem., Int. Ed.*, 2009, **48**, 1378.

2 (*a*) L. C. Gomes-da-Silva, N. A. Fonseca, V. Moura, M. C. Pedroso de Lima, S. Simões and J. N. Moreira, *Acc. Chem. Res.*, 2012, **45**, 1163; (*b*) M. L. Patil, M. Zhang, S. Betigeri, O. Taratula, H. He and T. Minko, *Bioconjugate Chem.*, 2008, **19**, 1396; (*c*) D. Astruc, E. Boisselier and C. Ornelas, *Chem. Rev.*, 2010, **110**, 1857; (*d*) K. Itaka, N. Kanayama, N. Nishiyama, W. D. Jang, Y. Yamasaki, K. Nakamura, H. Kawaguchi and K. Kataoka, *J. Am. Chem. Soc.*, 2004, **126**, 13612; (*e*) M. Meyer, A. Philipp, R. Oskuee, C. Schmidt and E. Wagner, *J. Am. Chem. Soc.*, 2008, **130**, 3272; (*f*) M. D. Krebs, O. Jeon and E. Alsberg, *J. Am. Chem. Soc.*, 2009, **131**, 9204; (*g*) C. A. Hong, S. H. Lee, J. S. Kim, J. W. Park, K. H. Bae, H. Mok, T. G. Park and H. Lee, *J. Am. Chem. Soc.*, 2011, **133**, 13914; (*h*) O. Boussif, F. Lezoualc'h, M. A. Zanta, M. D. Mergny, D. Scherman, B. Demeneix and J. P. Behr, *Proc. Natl. Acad. Sci. U. S. A.*, 1995, **92**, 7297.

3 (*a*) W. M. Pardridge, *Expert Opin. Biol. Ther.*, 2004, **4**, 1103; (*b*) E. Song, P. Zhu, S. K. Lee, D. Chowdhury, S. Kussman, D. M. Dykxhoorn, Y. Feng, D. Palliser, D. B. Weiner, P. Shankar, W. A. Marasco and J. Lieberman, *Nat. Biotechnol.*, 2005, **23**, 709; (*c*) D. J. Gary, N. Puri and Y. Y. Won, *J. Controlled Release*, 2007, **121**, 64; (*d*) M. D. Krebs and E. Alsberg, *Chem.–Eur. J.*, 2011, **17**, 3054.

4 M. V. Yezhelyev, L. Qi, R. M. O'Regan, S. Nie and X. Gao, *J. Am. Chem. Soc.*, 2008, **130**, 9006.

5 (*a*) T. Tokatlian and T. Segura, *Wiley Interdiscip. Rev.: Nanomed. Nanobiotechnol.*, 2010, **2**, 305; (*b*) P. Guo, O. Coban, N. M. Snead, J. Trebley, S. Hoeprich, S. Guo and Y. Shu, *Adv. Drug Delivery Rev.*, 2010, **62**, 650.

6 (*a*) H. Ding, K.-T. Yong, I. Roy, H. E. Pudavar, W. C. Law, E. J. Bergey and P. N. Prasad, *J. Phys. Chem. C*, 2007, **111**, 12552; (*b*) A. C. Bonoiu, S. D. Mahajan, H. Ding, I. Roy, K.-T. Yong, R. Kumar, R. Hu, E. J. Bergey, S. A. Schwartz and P. N. Prasad, *Proc. Natl. Acad. Sci. U. S. A.*, 2009, **106**, 5546.

7 I. B. Kim, A. Dunkhorst, J. Gilbert and U. H. F. Bunz, *Macromolecules*, 2005, **38**, 4560.

8 D. T. McQuade, A. E. Pullen and T. M. Swager, *Chem. Rev.*, 2000, **100**, 2537.

9 S. W. Thomas, G. D. Joly and T. M. Swager, *Chem. Rev.*, 2007, **107**, 1339.

10 I. B. Kim, H. Shin, A. J. Garcia and U. H. F. Bunz, *Bioconjugate Chem.*, 2007, **18**, 815.

11 J. H. Moon, W. McDaniel, P. MacLean and L. E. Hancock, *Angew. Chem., Int. Ed.*, 2007, **46**, 8223.

12 R. L. McRae, R. L. Phillips, I. B. Kim, U. H. F. Bunz and C. J. Fahrni, *J. Am. Chem. Soc.*, 2008, **130**, 7851.

13 A. Bajaj, O. R. Miranda, R. Phillips, I. B. Kim, D. J. Jerry, U. H. F. Bunz and V. M. Rotello, *J. Am. Chem. Soc.*, 2010, **132**, 1018.

14 (*a*) O. R. Miranda, C. C. You, R. Phillips, I. B. Kim, P. S. Ghosh, U. H. F. Bunz and V. M. Rotello, *J. Am. Chem. Soc.*, 2007, **129**, 9856; (*b*) M. D. Disney, J. Zheng, T. M. Swager and P. H. Seeberger, *J. Am. Chem. Soc.*, 2004, **126**, 13343; (*c*) Q. Zhou and T. M. Swager, *J. Am. Chem. Soc.*, 1995, **117**, 12593; (*d*) I. B. Kim, B. Erdogan, J. N. Wilson and U. H. F. Bunz, *Chem.–Eur. J.*, 2004, **10**, 6247; (*e*) I. B. Kim and U. H. F. Bunz, *J. Am. Chem. Soc.*, 2006, **128**, 2818.

15 L. Zhang, Q. H. Yin, H. Y. Huang and B. X. Wang, *J. Mater. Chem. B*, 2013, **1**, 756.

16 N. Cao, D. Cheng, S. Zou, H. Ai, J. Gao and X. Shuai, *Biomaterials*, 2011, **32**, 2222.

17 P. Chan, M. Kurisawa, J. E. Chung and Y. Yang, *Biomaterials*, 2007, **28**, 540.

18 Y. Wang, S. Gao, W.-H. Ye, H. S. Yoon and Y.-Y. Yang, *Nat. Mater.*, 2006, **5**, 791.

19 H. Peng, C. Soeller and J. Travas-Sejdic, *Chem. Commun.*, 2006, 3735.

20 Q. L. Fan, Y. Zhou, X. M. Lu, X. Y. Hou and W. Huang, *Macromolecules*, 2005, **38**, 2927.